The Influence of the Atmosphere on Curing Concrete Temperatures and Maturity

by

Gary S. Wojcik
Building and Fire Research Laboratory
National Institute of Standards and Technology
Gaithersburg, MD 20899 USA

Reprinted from the Advances in Cement and Concrete. Proceedings. Engineering Conferences International. Copper Mountain, CO, August 10-14, 2003, 491-500 pp., 2003.

NIST
National Institute of Standards and Technology
Technology Administration, U.S. Department of Commerce

THE INFLUENCE OF THE ATMOSPHERE ON CURING CONCRETE TEMPERATURES AND MATURITY

Gary S. Wojcik, NIST/NRC Post-doctoral Research Associate
National Institute of Standards and Technology
100 Bureau Drive Mailstop 8615
Gaithersburg, MD 20899
T: 1-301-975-8514; F: 1-301-990-6891; E: gwojcik@nist.gov

ABSTRACT

The SLABS model for the simulation of curing concrete bridge decks was developed with new boundary condition formulations that can accurately account for a wide variety of atmospheric conditions, addressing limitations of previous studies. Equivalent ages, estimated from the temperature predictions of SLABS, can vary up to 40 h over the conditions simulated after 24 h of hydration. Depth variations of equivalent ages reach 15 h.

INTRODUCTION

Ambient atmospheric conditions interact with the exothermic, temperature-dependent hydration reactions of concrete's binder components. This interaction may produce adverse high or low concrete temperatures and high temperature gradients, or insufficient concrete moisture content, perhaps resulting in cracking, reduced strength, or compromised long-term durability (e.g., 1,2). This interaction may also result in serious construction site safety problems. For example, the partial collapses of the Skyline Plaza Apartments in Fairfax County, VA in March 1973 (3) and a cooling tower in Willows Island, WV in 1978 (4), which resulted in the deaths of 14 and 51 workers, respectively, were attributed in part to low air temperatures that delayed concrete strength development.

Accurate predictions of concrete temperatures, temperature gradients, and moisture contents would provide engineers and field personnel with information they may need to make decisions about the proper time to place concrete or the proper time to continue the construction process. Such information would help to maintain safety of the construction site and ensure that high quality concrete is developed. Previous modeling studies of curing concrete exposed to the atmosphere did not use boundary conditions that could accurately account for a wide range of atmospheric conditions (e.g., 5).

In this study, the SLABS (SUNY Local Atmosphere Bridge Simulation) model is used to predict the temperatures and moisture content of curing concrete bridge decks containing New York State Department of Transportation's (NYSDOT) Class HP concrete, over a wide range of atmospheric conditions. The model boundary

conditions include explicit formulations for sensible heat convective, evaporative, net radiative, runoff spray water, and conductive heat fluxes (Fig. 1) developed from field investigations of the energy balances of curing concrete bridge decks (6). The temperature predictions are used to compute values of the maturity index, the equivalent age, as a function of atmospheric conditions. Such information provides the first comprehensive view of the effects of a wide range of atmospheric conditions on the equivalent ages of early-age concrete. The equivalent age can be related to concrete strength using a previously established relationship for the concrete being used.

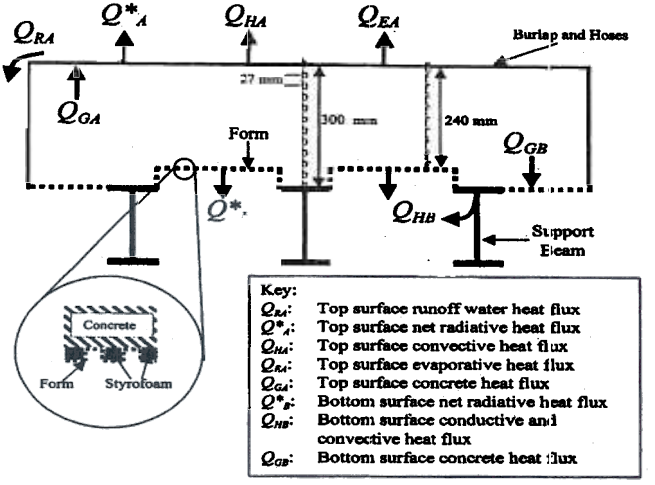

Fig. 1. Schematic cross-section of a bridge deck indicating the energy balance terms used as boundary conditions in the SLABS model. Not to scale. The arrows indicate the typical direction of energy flow when the peak concrete temperatures occur at night. "b" and "f" indicate grid points above a beam and above a form, respectively.

The maturity concept for estimating concrete strength is based on the idea that nominally identical specimens of concrete will acquire equal strength if they acquire equal values of a maturity index. For example, the equivalent age, t_e, is defined as the length of time at a specified temperature required to produce a maturity equal to the maturity achieved by a curing period at temperatures different from the specified temperature (7) and is given by:

$$t_e = \sum e^{-\frac{E_a}{R^*}\left(\frac{1}{T_c}-\frac{1}{T_s}\right)} \Delta t \qquad (1)$$

where E_a (J mol^{-1}) is the activation energy, R^* (8.314 J K^{-1} mol^{-1}) is the ideal gas constant, T_c (K) is the average temperature of the concrete during the time interval, Δt (h), and T_s is the specified or reference temperature (K). To use t_e as an indicator of strength development, it is assumed that the initial rate of strength development obeys the Arrhenius equation and that there is sufficient water available for hydration. To implement Eq. (1), it is necessary to know the value of E_a for concrete and T_s must be selected. Traditionally, T_s = 293 K has been used (8) and this value is chosen for this study.

ANALYTICAL INVESTIGATIONS WITH THE SLABS MODEL

Governing Equations

Below is a brief description of the portions of the SLABS model pertinent to the present work. For an expanded view of model details and performance, see (9). The SLABS model is a 1D (vertical) finite-difference model designed to study the heat transfer and generation and moisture movement in curing concrete bridge decks. The concrete bridge decks we studied are ≈ 60 mm thicker over the steel support "I" beams (300 mm deep) than they are over the "form" (a corrugated, galvanized steel sheet) (Fig. 1). The model consists of 10 vertical grid points (9 layers) above the form and 12 vertical grid points (11 layers) above the beams with a grid size of 27 mm. For the bridges studied, moist curing of the decks with burlap and spray water from irrigation hoses was used. We focus only on simulations over the form in the present study.

The concrete simulated for this study is New York State Department of Transportation's (NYSDOT) Class HP mixture whose binder component has mass fractions of 74 % ASTM Type I, Type II, or Type I/II cement, 20 % Class F flyash and 6 % silica fume (10). Class HP concrete has a water to binder ratio (*w/b*) of 0.38. The hydration reactions are modeled as a bimolecular reaction between the binder and the water (11).

The change in the unhydrated binder concentration, B, ($mol_B\ m^{-3}$) is given by:

$$\frac{dB}{dt} = -k \cdot B^n \cdot R^m \tag{2}$$

where R ($mol_R\ m^{-3}$) is the concentration of water available for the hydration reactions; n and m are exponents whose sum gives the order of the hydration reaction; k ($m^3\ mol_R^{-1}\ s^{-1}$) is the reaction rate constant given by:

$$k = A \cdot \exp\left(-\frac{E_a}{R^* \cdot T_c}\right) \tag{3}$$

where A is the pre-exponential factor and T_c (K) is the concrete temperature. Wojcik et al. (11) determined n=m=1 and E_a=35 kJ mol^{-1} for Class HP binder and Wojcik et al. (9) determined A=0.0039. Note that this E_a is used also in Eq. (1).

The governing equation for concrete temperature, T_c, is given by:

$$\frac{dT_c}{dt} = K_T \frac{\partial^2 T_c}{\partial z^2} - V \cdot \frac{dB}{dt} \tag{4}$$

where the second term on the right hand side of Eq. (4) is the hydration heat source term where the parameter, V (K m^3 mol_B^{-1} s), converts the reacted binder concentration to heat and is equal to $-\Delta H^* M_{wB}/\rho_c c_{pc}$; $-\Delta H$: the Class HP concrete heat of hydration (~420 kJ kg^{-1}); c_{pc}: the specific heat capacity of Class HP concrete (1380 J kg^{-1} K^{-1}); and ρ_c: the density of Class HP concrete (2230 kg m^{-3}). K_T is the thermal diffusivity of concrete (8.8×10^{-7} m^2 s^{-1}), from ρ_c, c_{pc}, and the Class HP thermal conductivity k_c (2.7 W m^{-1} K^{-1}) (6,11). M_{wB} is the molecular weight of the binder (~0.2 kg mol^{-1}) determined from a mass average weighting of the molecular weights of cement, flyash and silica fume.

The change in available water concentration, R ($mol_R\ m^{-3}$), is given by:

$$\frac{dR}{dt} = K_R \frac{\partial^2 R}{\partial z^2} + \eta \cdot \frac{dB}{dt} \tag{5}$$

where K_R is the diffusivity of water in concrete (12) and changes as a function of hydration fraction. R is the water concentration in the concrete that is available for the hydration reactions. The term, η, represents the number of moles of water removed from the available water per mole of binder that hydrates. This term includes water that is chemically converted into hydration products and water that is adsorbed onto the surface of the hydration products where it cannot be used for further hydration (13). Wojcik et al. (9) determined η=8.3.

Boundary conditions

By convention, upward fluxes are positive. At the top surface, the energy balance ($W\ m^{-2}$) is given by:

$$-Q_A^* + Q_{GA} = Q_{EA} + Q_{HA} + Q_{RA} \tag{6}$$

where $-Q^*_A$ is the net radiation (net shortwave + net longwave); Q_{GA} is the heat flux through the top surface of the concrete; Q_{HA} is the convective sensible heat flux; Q_{EA} is the evaporation heat flux; and Q_{RA} is the runoff water heat flux (Fig. 1).

The total top surface energy flux is explicitly given by:

$$Q_{GA} = -k_c \frac{dT_c}{dz} =$$

$$Q_A^* - \rho L_v CU(q_a - q_s) - \rho c_p CU(T_a - T_s) - \rho_w c_w (T_{wi} - T_{wf}) \frac{M}{A_{top}} \tag{7}$$

The second term on the right hand side of Eq. (7) is the evaporative heat flux, the third is the sensible heat flux, and the fourth is the runoff water heat flux. M is the volume flow rate of spray water running off the bridge ($m^3\ s^{-1}$); A_{top} is the area of the bridge's top surface (m^2); q_a and q_s are the air and surface specific humidities ($g_w\ g_a^{-1}$); T_a and T_s are the air and surface temperatures (°C); ρ_w and ρ are the water and air densities ($kg\ m^{-3}$); c_w and c_p are the water and air specific heat capacities ($J\ kg^{-1}\ K^{-1}$); L_v is the latent heat of evaporation ($J\ kg^{-1}$); U is the wind speed ($m\ s^{-1}$); C is the dimensionless exchange coefficient; z is the vertical dimension (m); and T_{wi} and T_{wf} are the initial (when hitting the top surface) and final (when running off the bridge) spray water temperatures (°C).

For conditions other than free convection (free convection is assumed when the atmospheric stability indicator, the bulk Richardson number, Rb, < -1 (14) and U < 1 $m\ s^{-1}$), the exchange coefficients were determined by Wojcik and Fitzjarrald (6). Free convection exchange speeds (equal to CU in Eq. (7)) are given by Kondo and Ishida (15) for a smooth surface.

The net radiation is computed by determining the incoming and outgoing longwave and shortwave radiation components with schemes given by Stull (14), Freedman et al. (16), Prata (17), and Brutsaert (18).

The spray water drops will adjust to the environmental conditions as they rise and fall after being ejected from the irrigation hoses. Because the drops do not remain airborne for more than a few seconds, their temperatures generally do not approach the air wet-bulb temperature. A model by Pruppacher and Klett (19) is used to calculate the temperature of the spray water as it hits the top surface (T_{wf}).

At the sheet metal form, the heat flux at the bridge deck bottom, Q_{GB} (W m^{-2}), is given by:

$$Q_{GB} = -k_c \frac{dT_c}{dz} = Q_B^* + \rho c_p U C_b (T_a - T_{cf}) \quad (8)$$

where the second term on the right-hand side accounts for convective heat loss; T_{cf} is the temperature of the form; Q^*_B is the net radiation at the bottom surface; and C_b is the exchange coefficient for the form. To model the heat transfer through the steel support beams (Fig. 1), a formulation of heat flow through an infinite steel fin (20) is used.

Boundary condition sensitivity studies

We calculated the equivalent ages of concrete for a wide variety of atmospheric and construction conditions for the first 24 h of the active phase of the hydration reactions. The equivalent ages were computed using Eq. (1) starting at the end of the induction period of the hydration reactions and the concrete was allowed to mature as long as there was water available for reaction at a given point. The atmospheric variables considered were air temperature and relative humidity (T_a and RH), wind speed (U), and cloud cover fraction (clf) which affects radiation (16). The range of values chosen represents typical atmospheric conditions. Diurnal variations of the atmospheric variables were approximated with simple cosine functions that capture the main features of typical diurnal variations (9). T_a and U generally peak during the late afternoon while RH reaches a minimum during this time. The simulations were run for Albany, NY in early June with the concrete being placed at 0700 local time (LT). The length of the induction period of the hydration reactions was set at eight hours.

RESULTS

Equivalent age sensitivity to atmospheric conditions

When averaged over the Class HP deck slab, concrete temperatures and equivalent ages, t_e, are maximum when the curing concrete was influenced by high air temperatures and humidities (Figs. 2 and 3). Under these conditions, evaporation and convection are limited, allowing the concrete to retain heat. The average equivalent ages at 24 h varied between 18 h and 55 h (Fig. 3).

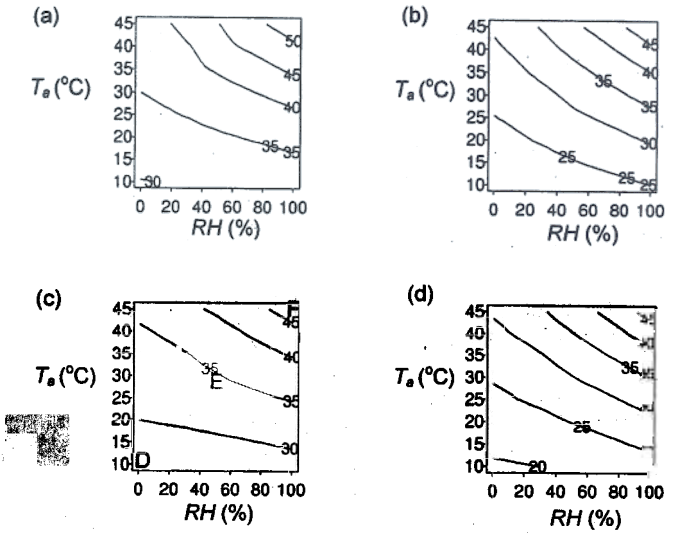

Fig. 2. a) Contours of predicted concrete temperatures averaged over the slab thickness over the period of time used to compute the equivalent ages, as a function of afternoon *RH* and T_a, with $U = 0.5$ m s^{-1} and *clf* = 0. b) as in (a), but with $U = 5$ m s^{-1}. c) as in (a), but with *clf* = 1. d) as in (a), but with $U = 5$ m s^{-1} and *clf* = 1.

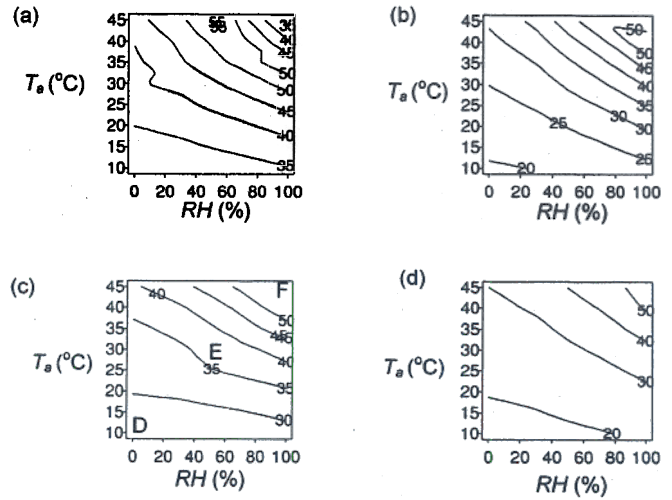

Fig. 3. a) Contours of predicted equivalent ages at 24 h after the induction period averaged over the slab thickness as a function of afternoon *RH* and T_a, with $U = 0.5$ m s^{-1} and *clf* = 0. b) as in (a), but with $U = 5$ m s^{-1}. c) as in (a), but with *clf* = 1. d) as in (a), but with $U = 5$ m s^{-1} and *clf* = 1.

Note in Fig. 3a that t_e are reduced at the highest air temperatures and humidities. For these simulations, with low wind speeds, the convective and evaporative heat fluxes are low which allows the concrete temperatures to reach their maximum (reaching a peak of 64 °C) near the bottom of the concrete slab. With such high temperatures, the hydration is extremely rapid, very quickly using up the water available for hydration. Since water from the top surface does not penetrate below the top 2 or 3 grids (9), the mix water is not replenished. With no available water, the concrete cannot continue to mature, resulting in lower equivalent ages when averaged over the slab thickness. While this self-desiccation has not been verified directly for Class HP concrete, it is possible given that Class HP contains 24 % cement replacement with flyash and silica fume (e.g., 21). Note that if it is assumed that there is sufficient water under these conditions, t_e continues to increase smoothly as T_a and RH increase and reaches a peak of 70 h.

Increasing the wind speed and the cloud cover fraction lowers the equivalent ages, with the wind speed having the larger effect of these two variables. For example, increasing the wind speed from 0.5 m s^{-1} to 5 m s^{-1} lowers the equivalent age from 32 h to 19 h for T_a = 10 °C, RH = 0 %, and clf = 0 (Figs. 3a and 3b). Increasing the cloud cover fraction from clf = 0 to clf = 1, lowers t_e from 32 h to 26 h at T_a = 10 °C, RH = 0%, and U = 0.5 m s^{-1} (Figs. 3a and 3c). Higher wind speeds allow more efficient convective and evaporative heat loss, lowering concrete temperatures and so the equivalent ages. Increasing the cloud cover fraction reduces incoming solar radiation producing lower concrete temperatures and equivalent ages.

Vertical profiles of equivalent ages

While the above results show that t_e averaged over the slab thickness can vary widely depending on ambient conditions, t_e can also vary with depth within the slab under given conditions (Fig. 4). The vertical profiles in Fig. 4 are for points indicated by "D", "E", and "F" in Figs. 2c and 3c. In general, the equivalent ages decrease with distance above the form and are maximum near the bottom of the slab where concrete temperatures are maximum. For the T_a and RH sensitivity simulations reported here, t_e varies by up to 15 h from bottom to top. Because up to 85 % of the heat transfer occurs at the top surface of bridge decks (6), lowest temperatures, and largest temperature and t_e gradients occur near the top surface.

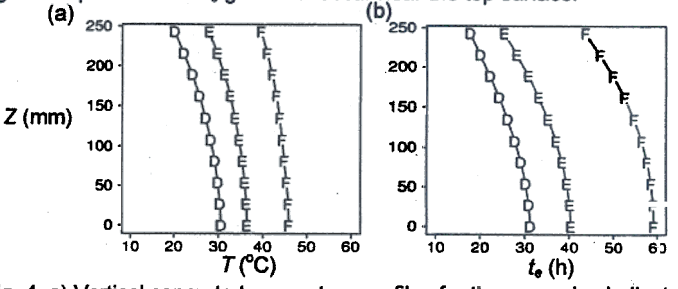

Fig. 4. a) Vertical concrete temperature profiles for the scenarios indicated in Fig. 2c by "D", "E", and "F". Z gives the distance above the form. b) Vertical profiles of equivalent ages for the scenarios indicated in Fig. 3c by "D", "E", and "F".

SUMMARY AND CONCLUSIONS

In this paper, we have applied the SLABS model to investigate the influence of atmospheric conditions on the equivalent ages of concrete bridge decks at 24 h after the induction period with the following important findings:

1. As long as there is sufficient water available for hydration, the maximum equivalent ages coincide with the maximum concrete temperatures. Self-desiccation, especially deep within the slab, must be considered when determining concrete maturity of high performance mixes containing pozzolans under extreme environmental conditions. Note that self-desiccation is also a function of the water binder (*w/b*) ratio.
2. As expected, equivalent ages after 24 h of hydration averaged over the entire slab thickness are maximum under conditions of high air temperatures and relative humidities and low wind speeds.
3. Over the ranges of variables tested, equivalent ages can vary from less than 20 h to more than 50 h after 24 h of hydration.
4. The variations of equivalent ages with depth can approach 15 h with the maximum values generally occurring near the bottom of the slab where the maximum concrete temperatures developed.

The results from this investigation show clearly that many factors are involved in controlling NYSDOT Class HP concrete temperatures and maturity. At early ages, small differences in equivalent ages can represent large differences in concrete strength. Therefore, not only must the field engineer decide the time of placement and the curing regimen for a concrete structure, the engineer must also pay close attention to the atmospheric conditions that are expected to ensure that the structure attains the proper maturity at the time of critical construction operations.

Because other concrete mixtures may have different sensitivities to environmental conditions, the results presented here should be viewed as the first attempt to examine such sensitivities, but specific to Class HP concrete. Moreover, while a wide variety of conditions were simulated for this study, they are a subset of what can occur and therefore, care must be taken when applying the results presented here to other situations.

The engineer must consider the effect of depth variations of maturity in a concrete structure. Such variations become important when attempting to determine the overall maturity of a concrete element by a single point measurement. While some portions of the concrete may have reached the specified strength needed for continuing construction or opening a slab to traffic, other portions may have not reached the proper strength. Recognizing this depth variation may be necessary to maintain construction site and public safety. Because most heat transfer and the lowest temperatures occur near the top surface, sampling with a maturity meter near the top surface generally will indicate the lowest maturity attained by the slab, information that will provide a lower limit to the strength development.

The SLABS model indicates that self-desiccation of Class HP concrete may occur under some extreme conditions especially deep within the slab at early ages. Accounting for this self-desiccation when computing maturity indices will lower their value as the results show. Moist curing may provide water to the uppermost 50 mm

of the slab, but this water probably does not influence hydration below this level (e.g., 2, 22). Current research by the author with an X-ray absorption system at the National Institute of Standards and Technology seeks to determine more rigorously this depth of influence as a function of *w/b*, curing regimen, and materials. There is a need to determine under what conditions and for what mixture proportions such desiccation may occur so that its effect on concrete maturity can be taken into account.

Other factors such as time of placement, initial concrete temperature, and spray water volume and temperature will also influence the concrete's temperature and maturity (9, 23). These factors, then, could be used to offset any problems that could arise due to adverse atmospheric conditions. For example, the initial concrete temperature of a batch of concrete could be lowered to counter the effects of high ambient air temperatures or low wind speeds on concrete temperatures. A simplified field model, such as SLABS, that accounts for all of these factors in predicting concrete temperatures could be an important tool for determining the expected concrete maturity and temperatures on a case by case basis. Such a tool could aid in developing the best quality concrete and maintaining the safety of the construction site, perhaps preventing future disasters such as those at the Skyline Plaza Apartments in Fairfax County, VA and the Willows Island cooling tower.

ACKNOWLEDGEMENTS

The author gratefully acknowledges the funding support of the NIST/NRC Post-doctoral Research Associateship Program. The author wishes to thank the Inorganic Materials Group of the Materials and Construction Research Division in the Building and Fire Research Laboratory at NIST for their support in making this research possible.

REFERENCES

(1) Gopalan, M. K., and M. N. Haque (1987). "Effect of curing regime on the properties of fly-ash concrete." *ACI Materials Journal*, **84** (1), 14-19.
(2) Neville, A. M. (1996). *Properties of Concrete*. Wiley & Sons, 844 pp.
(3) Carino, N. J., K. A. Woodward, E.V. Leyendecker, and S. G. Fattal (1983). "A review of the Skyline Plaza collapse." *Concrete International*, **7**, 35-42.
(4) Lew, H. S. (1980). "America's worst construction accident: part one." *Civil Engineering ASCE*, **2**, 1-6.
(5) Kapila, D., J. Falkowsky, and J. L. Plawsky (1997). "Thermal effects during curing of concrete pavements." *ACI Materials Journal*, **94** (2), 119-128.
(6) Wojcik, G. S., and D. R. Fitzjarrald (2001). "Energy balances of curing concrete bridge decks." *Journal of Applied Meteorology*, **40** (11), 2003-2025.
(7) ASTM (1999). "ASTM C 1074-98 Standard specifications for estimating concrete strength by the maturity method." *Annual Book of ASTM Standards, Vol. 04.02.*
(8) Freiesleben Hansen, P. and J. Pederson (1977). "Maturity computer for controlled curing and hardening of concrete." *Nordisk Betong*, **1**, 19-34.
(9) Wojcik, G. S., D. R. Fitzjarrald, and J. L. Plawsky (2003). 'Modeling the interaction between the atmosphere and curing concrete bridge decks with the SLABS model." *Meteorological Applications*, in press.
(10) NYSDOT (1999). "Specification revisions-Class HP concrete for substructures and structural slabs." NYSDOT Rep. EI 99-002, 22 pp. [Available from New York

State Department of Transportation Structures Division, 1220 Washington Ave., Building 5, 6th floor, W. Averell Harriman State Office Building Campus, Albany, NY, 12232-0600.]

(11) Wojcik, G. S., J. L. Plawsky, and D. R. Fitzjarrald (2001). "Development of a bimolecular expression to describe the heat generation of Class HP concrete." *Cement and Concrete Research*, **31** (12), 1847-1858.

(12) Pommersheim, J. M., and J. R. Clifton (1991). "Models of transport processes in concrete. National Institute of Standards and Technology Internal Report NISTIR 4405." 92 pp.

(13) Powers, T. C. and T. L. Brownyard (1946-1947). "Studies of physical properties of hardened Portland cement paste (nine parts)." Journal of the American Concrete Institute, **43**.

(14) Stull, R. B. (1988). *An Introduction to Boundary Layer Meteorology.* Kluwer Academic Press, 666 pp.

(15) Kondo, J., and S. Ishida (1997). "Sensible heat flux from the Earth's surface under natural convection conditions." *Journal of the Atmospheric Sciences*, **54**, 498-509.

(16) Freedman, J. M., D. R. Fitzjarrald, K. E. Moore, and R. K. Sakai (2001). "Boundary layer clouds and vegetation-atmosphere feedbacks." *Journal of Climate*, **14**, 180-197.

(17) Prata, A. J. (1996). "A new long-wave formula for estimating downward clear-sky radiation at the surface." *Quarterly Journal of the Royal Meteorological Society*, **122**, 1127-1151.

(18) Brutsaert, W. (1975). "On a derivable formula for longwave radiation from clear skies." *Water Resources Research*, **11**, 742-744.

(19) Pruppacher, H. R., and J. D. Klett (1997). *Microphysics of Clouds and Precipitation.* Kluwer Academic Publishers, 954 pp.

(20) Incropera, F. P., and D. P. DeWitt (1996). *Introduction to Heat Transfer*, John Wiley & Sons, 801pp.

(21) Hooton, R. D. (1993). "Influence of silica replacement of cement on physical properties and resistance to sulfate attack, freezing and thawing, and alkali-silica reactivity." *ACI Materials Journal*, **90** (2) 143-151.

(22) Bentz, D. P. (2002). "Influence of curing conditions on water loss and hydration in cement pasts with and without flyash substitution." National Institute of Standards and Technology Internal Report NISTIR 6886, 15 pp.

(23) Wojcik, G. S. (2003). "The effects of atmospheric and construction conditions on curing concrete equivalent ages." submitted to *ACI Materials Journal.*